Polymer 51 (2010) 2084–2090

Contents lists available at ScienceDirect

Polymer

journal homepage: www.elsevier.com/locate/polymer

Study on the structure and properties of SSBR with large-volume functional groups at the end of chains

Lei Wang [a], Suhe Zhao [a,b,*], An Li [a], Xingying Zhang [a,b]

[a] Key Laboratory of Beijing City on Preparation and Processing of Novel Polymer Materials, Beijing 100029, China
[b] Key Laboratory for Nanomaterials, Ministry of Education, Beijing University of Chemical Technology, Beijing 100029, China

ARTICLE INFO

Article history:
Received 9 November 2009
Received in revised form
3 February 2010
Accepted 2 March 2010
Available online 7 March 2010

Keywords:
Solution polymerized styrene-butadiene rubber (SSBR)
Dispersions
End-capping modification

ABSTRACT

Solution polymerized styrene-butadiene rubber (SSBR) and SSBR with tert-Butylchlorodiphenylsilane (TBCSi, large-volume functional groups) at the two ends of macromolecular chains (T-SSBR) were prepared by anionic polymerization. The molecular structure parameters of T-SSBR and SSBR were characterized and the ratio of the amount of macromolecular chain ends connected with TBCSi to total macromolecular chain ends (i.e., end-capping efficiency) was calculated. The comprehensive properties of T-SSBR and SSBR composites filled with carbon black (CB) were investigated. The results showed that T-SSBR composites presented lower Payne effect (namely better CB dispersion) than those of SSBR composites, which led to decrease in hardness, internal friction, dynamic compression heat built-up and permanent set of T-SSBR composites, significant increase in tensile strength, elongation at break, tear strength and resilience of T-SSBR composites, and excellent balance between wet-skid resistance and rolling resistance. However, compared with SSBR composites, T-SSBR composites presented longer stress-relaxation time, bigger die-swell and higher apparent viscosity, as well as slightly inferior dynamic-cutting resistance. All the above, owing to the end-capping of TBCSi, which could immobilize the free chain ends of T-SSBR (i.e., to reduce the friction loss of molecular chains and create a greater degree of orientation in the force field), and adsorb CB, the comprehensive performances of T-SSBR were better than those of SSBR and T-SSBR terminated with styrene-TBCSi (T_S-SSBR) were far superior to those of T-SSBR terminated with butadiene-TBCSi (T_B-SSBR). Accordingly, the former was suitable for the tread of green tires.

1. Introduction

In recent years, in response to the rapid development of the car industry, the increasing shortage of oil resources and ever more demanding requirements from the environmental protection, the requirements for high-performance tires with long service life, safety and energy-saving properties have been more strict, which requires the tread compounds with better wear resistance, higher wet-skid resistance and lower rolling resistance respectively [1,2]. However, the three desired properties of the high-performance tires are hard to be improved simultaneously. Especially for lower oil consumption of the green tires, it is difficult to achieve through the conventional combination of emulsion polymerized styrene-butadiene rubber (ESBR), cis-butadiene rubber (BR) and natural rubber (NR). Therefore, it is necessary to develop solution polymerized styrene-butadiene rubber (SSBR) with not only lower heat built-up, but also higher gripping behavior, wear resistance and flex resistance in order to adapt to the situation [3,4].

In view of structural analysis SSBR has the same styrene content (St %) as ESBR and a higher vinyl content (Bv %) than that of ESBR. It has been found that the gripping behavior, wear resistance and mechanical properties of SSBR are similar with or higher than those of ESBR. Meanwhile, SSBR with proper structure could exhibit the energy-saving properties. Therefore SSBR is usually used to make green tire treads. The modification of SSBR can be carried out through controlled/"living" polymerization, which makes the methods of molecular structure modification diversified [5–8]. Among these, the modification of the molecular chain ends is the principal means endowing SSBR with energy-saving properties (i.e., both hysteresis loss and heat build-up are decreased via reducing the amount of free chain terminals) [9]. Currently, controlled/"living" anionic polymerization has been adopted to perform end modification of SSBR. The end modification technologies mainly include Sn-coupled and end-group functionalized modification.

* Corresponding author at: Key Laboratory for Nanomaterials, Ministry of Education, Beijing University of Chemical Technology, Beijing 100029, China. Tel.: +86 10 64456158; fax: +86 10 64433964.
E-mail addresses: Zhaosh@mail.buct.edu.cn, 13671396057@139.com (S. Zhao).

0032-3861/$ – see front matter © 2010 Published by Elsevier Ltd.
doi:10.1016/j.polymer.2010.03.006

Sn-coupled SSBR is one of the typical products obtained by end modification technologies. JSR and Zeon Corporation of Japan etc. have produced a few varieties of partly coupled SSBR [10–16], which have remarkable energy saving. Since parts of macromolecular chain terminals are coupled by Sn, the internal friction caused by the random thermal motion of the chain terminals is reduced. Recently, Beijing University of Chemical Technology [17,18] has invented a novel multi-lithium initiator, by which a fully-coupled SSBR with low hysteresis loss is prepared through one-step synthesis technique. This kind of rubber has been produced at a pilot-scale plant and used in high-speed passenger-car tires [19], which is popular with the tire manufacturers.

The chain-end functionalized modification of SSBR includes reactive functional group and large-volume functional group end-capping technologies. The former could react and bond with the active groups on the nano-filler surface. The latter could immobilize the free chain ends. Xiaolin Li et al. [20,21] has used 3-chloropropyl trimethoxy siloxane to react with C^- at the end of SSBR macromolecule chains to make SSBR with trimethoxy silane at the two ends. It is easy to provoke grafting reaction on SiO_2 surface and the SSBR/SiO_2 composites has not only improved the filler dispersion, but also decreased the internal friction. Bridgestone Corporation, Japan [22] has prepared a polymer modified by N-(1,3-dimethylbutylidene)-3-(diethoxy silyl)-1-propylamine at the molecular chain ends. The fillers dispersed well in the modified polymer, which results in the great improvement of the tensile strength, abrasion and wet-skid resistance as well as low heat built-up of the composites. Eunkyoung Kim et al. [23] have prepared a polar polydimethylsiloxane terminator, which could react with living anion in copolymer of styrene-butadiene, to synthesize SSBR modified by the reactive-functional-group at the chain ends. The obtained SSBR/SiO_2 composite exhibits lower tan δ at 60 °C and higher tan δ at 0 °C than SSBR-Sn/SiO_2 composite. The end-capping modification with large-volume functional groups is a novel direction for preparing energy-saving SSBR by means of molecular design and synthesis. However, there are very few reports on this aspect.

In this work, a kind of SSBR and three kinds of T-SSBR (SSBR end-capped by tert-Butylchlorodiphenylsilane (TBCSi)) were prepared by anionic polymerization, their molecular structure parameters were characterized and the end-capping efficiency of T-SSBR was calculated. Stress relaxation, rheological properties, mechanical properties, dynamic mechanical properties, dynamic cutting resistance and dynamic compression heat built-up of the three kinds of T-SSBR composites were investigated, and their morphological structure were observed by TEM, and compared with those of SSBR composites. It is expected that these experimental results could provide some theoretical and practical basis for the design and synthesis of energy-saving rubbers used in green tires.

2. Experimental section

2.1. Materials

Cyclohexane (industrial grade), Styrene (St) (analysis grade) and methanol (analysis grade) were all produced by Beijing Chemical Reagents Company (Beijing, China). Butadiene (Bd) (polymerization grade) was provided by Beijing Yanshan Petrochemical Corporation (Beijing, China). Tetrahydrofuran (THF) (analysis grade) was produced by Beijing Chemical Works (Beijing, China). Bifunctional organic lithium initiator was self-prepared. Tert-Butylchlorodiphenylsilane (TBCSi) (purity: 98%) was produced by J&K Chemical Ltd (Beijing, China).

SSBR (A_1) and three kinds of T-SSBR (A_2, A_3, A_4) are all synthesized in our group. T_S-SSBR (A_2, A_3) were SSBR with a short chain made up of 3–5 styrene monomers at the macromolecular chain ends, and end-capped by TBCSi. T_B-SSBR (A_4) was SSBR with a short chain made up of about 10 butadiene monomers at the macromolecular chain ends, and end-capped by TBCSi. The Structural parameters of four kinds of samples are shown in Table 1.

Carbon black (N234) was produced by Tianjin Haitun Carbon Black Co., Ltd. (Tianjin, China); the other rubber additives were of commercial grade.

2.2. Formulation for preparing the rubber compounds

SSBR 100.0, N234 50.0, Zinc oxide 4.0, Stearic acid 2.0, 2,2,4-trimethyl-1,2-dihydroquinoline 1.5, N-cyclohexyl-2-benzothiazyl sulfenamide 1.0, Tetramethylthiuramdisulfide 0.2, Aromatic oil 5.0, Sulfur 1.8 (phr)[e]. [e] Parts-per-hundred rubber.

2.3. Specimen preparation

2.3.1. Preparation of SSBR samples

The purified cyclohexane, butadiene, styrene and THF were added into a 2L stainless reactor in proportion, which was purified with nitrogen gas and washed with living polystyryl-lithium solution beforehand. The polymerization was initiated by bifunctional organic lithium initiator, which had been prepared in advance. The temperature of the reactor was kept at 50 °C for 2–4 h. After the polyreaction was terminated, TBCSi was added into the polymerization solution of A_2, A_3 respectively to react for 1 h, and for A_4, before adding TBCSi, another small amount of butadiene was added into the polymerization solution to form a short chain at the macromolecular chain ends, and the polyreaction of A_1 sample was terminated by methanol. After end-capping reaction, the polymer was purified by precipitation with technical alcohol and dried in a vacuum oven. The dried products were dissolved in the solvent of cyclohexane and the unreacted TBCSi was extracted from the polymers using the technical alcohol again. At last the four kinds of polymer (A_1–A_4) were obtained after being dried to constant weight in the vacuum oven. A_1 was unmodified linear polymer (SSBR), A_2 and A_3 were linear SSBR terminated with 3–5 styrene unit-TBCSi (Ts-SSBR), and A_4 was linear SSBR terminated with about 10 butadiene unit-TBCSi (T_B-SSBR). The reaction mechanism of T-SSBR (Ts-SSBR and T_B-SSBR) is shown in Fig. 1.

2.3.2. Preparation of the rubber compounds

CB was mixed into rubber by an open two-roll mill (Shanghai Rubber Machinery Works No. 1, Shanghai, China). After the mixtures were thin-passing and well-mixed, other addition agents were successively added into them for further mixing. Finally the rubber compounds were sheeted and waited for future use.

2.3.3. Preparation of the vulcanizates

The vulcanizing properties of the compounds were determined by a P3555B_2 Disc Vulkameter (Beijing Huanfeng Chemical Machinery

Table 1
Structural parameters of SSBR and T-SSBR.

Compound no.	Mn (g/mol)	Mw (g/mol)	MWD	St[a] (%)	Bv[b] (%)	End type[c]	End-capping efficiency
A_1	131,000	185,000	1.40	20.8	48.0	St unit	0
A_2	117,000	159,000	1.35	20.6	47.3	St unit-TBCSi	0.54
A_3	157,000	224,000	1.42	21.0	48.7	St unit-TBCSi	0.51
A_4	197,000	278,000	1.38	20.2	50.3	Bd[d] unit-TBCSi	0.71

[a] Styrene content.
[b] The content of 1,2-butadiene structure.
[c] The two end groups of the SSBR molecular chains.
[d] Butadiene.

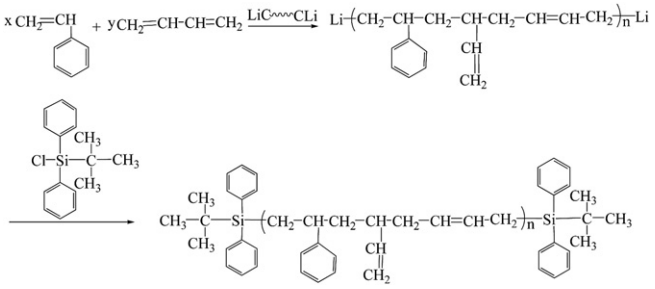

Fig. 1. Reaction mechanism of T-SSBR.

Trial Plant, Beijing, China) and then the vulcanizate samples were prepared by a XLB-D350 × 350-type Automatic Operation Vulcanizing Press (Huzhou Dongfang Machinery Co., Ltd, Zhejiang, China). The curing condition was 150 °C × t_{90} (optimum cure time).

2.4. Characterization

Chemical structure was detected by a Bruker AV600 spectrometer, produced by Bruker Co. Germany (600 MHz for ^{1}H NMR). The sample was dissolved in $CDCl_3$ in a 5 mm NMR tube and analyzed at room temperature. Chemical shifts were referenced to tetramethylsilane as internal standard and calculated by using the residual isotopic impurities of the deuterated solvents. All NMR chemical shifts are reported in ppm. The following parameters were used to acquire the ^{1}H NMR spectra: relaxation time = 2 s; acquisition time = 2.73 s; flip angle = II/4; number of transients = 16.

Stress relaxation was determined by RPA2000 Rubber Process Analyzer, produced by Alpha Technologies Co. US. The temperature was 100 °C, the strain was 70%, the preheat time was 300s and the test time was 120s. The stress-relaxation time (i.e., the time needed for the stress to decrease to 0.368 of the initial stress under constant strain and temperature) was determined.

Rheological properties were determined by an Instron 3211 Capillary Rheometer produced by Instron Co. UK. The length/diameter ratio of the capillary was 16:1 (without entrance correction), the piston velocity of the capillary was 0.06, 0.20, 0.60, 2.00, 6.00 and 20.00 cm/min respectively, the testing temperature was 90 °C and the preheat time was 10 min. The die-well characteristic was determined by a reading microscope. The die-swell ratio (B) was represented as B = d/D. Here d-extrudate diameter (mm); D-capillary diameter (mm).

Dynamic mechanical property (strain sweep) was determined by RPA2000 Rubber Process Analyzer, produced by Alpha Technologies Co. US. The testing temperature was 60 °C, the strain was varied from 0.28% to 42% and the frequency was 10Hz (vulcanizates).

Dynamic mechanical property (temperature sweep) was determined by VA3000 Dynamic Mechanical Thermal Analyzer, produced by 01dB-Metravib, France. Testing conditions: the temperature was from −100 °C to 100 °C, the speed of temperature rise was 3 °C/min, the frequency was 10Hz and the strain amplitude was 0.1% (operated in a rectangular tension mode).

Mechanical properties were measured according to ASTM D638 by CMT4104 Electrical Tensile Tester produced by Shenzhen SANS Test Machine Co., Ltd. China, at a tensile rate of 500 mm/min. Shore A hardness of the vulcanizates was measured with a rubber hardness apparatus produced by the 4th Chemical Industry Machine Factory Shanghai, China.

Resilience was determined with MZ-4065 Resilience Elasticity Tester produced by Mingzhu Testing Machinery Co., Ltd, China at 23 °C.

Dynamic cutting resistance was determined by RCC-I Rubber Dynamic Cutting Tester produced by Beijing Wanhui Yifang Technology Development Co., Ltd. China. The wheel speed was 720r/min, the hitting velocity was 120 n/min and the testing time was 20 min.

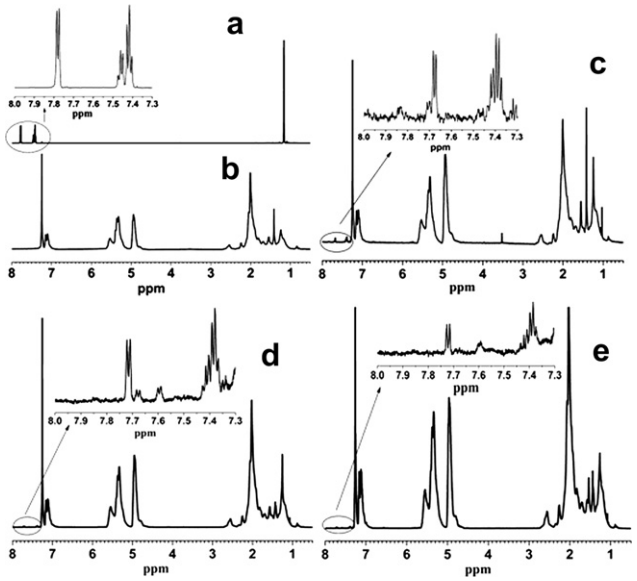

Fig. 2. ^{1}H NMR spectra of TBCSi (a), A_1 (b), A_2 (c), A_3 (d) and A_4 (e).

Dynamic compression heat was determined by YS-25 Compression Heat Built-up Tester, produced by Shanghai rubber machinery works, China. Testing conditions: the preheating time was 20 min, the compression time was 25min, the frequency was 1800min $^{-1}$, the stroke was 4.45 mm and the load was 1 MPa.

Morphological structure was observed by H-800-1 Transmission Electron Microscopy, produced by Hitachi Co. Japan. The acceleration voltage was 200KV. The thin sections were cut by microtome under −100 °C and collected on the cooper grids.

3. Results and discussion

3.1. The chemical structure and end-capping efficiency of T-SSBR

3.1.1. Chemical structure characterization

^{1}H NMR spectra curves of T-SSBR and SSBR are depicted in Fig. 2

In Fig. 2 (a) the characteristic peaks both at 7.76 ppm and 7.39–7.46 ppm represent proton (H) in benzene of TBCSi. Also the peak at 1.13 ppm represents H in tert-butyl of TBCSi. Usually the

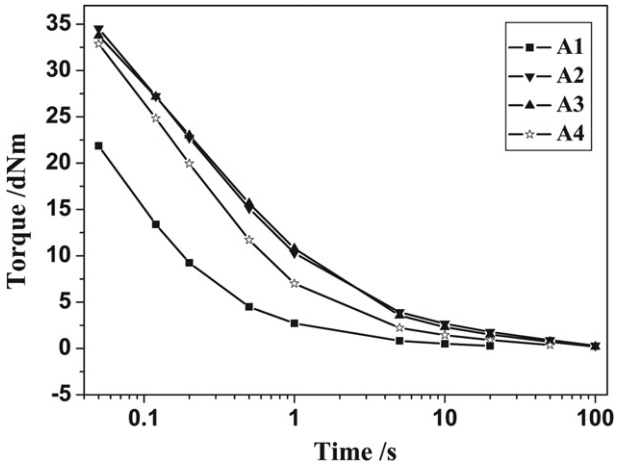

Fig. 3. The stress-relaxation curves of T-SSBR/CB and SSBR/CB compounds.

Table 2
The stress-relaxation time of T-SSBR/CB and SSBR/CB compounds.

Samples no.	A_1	A_2	A_3	A_4
Stress-relaxation time/s	0.072	0.249	0.267	0.177

resonance peaks between 6.20 and 6.85 ppm show the characteristic of block styrene. Therefore, in Fig. 2 (b), (c), (d) and (e) spectra, the absence of block styrene characteristic demonstrates that all the SSBR samples have random distribution of composition. H in benzene of SSBR appears as a doublet peaks between 7.09 and 7.17 ppm, which are different from those of H in benzene of TBCSi. Fig. 2 (c), (d) and (e) spectra display the characteristic peaks at 7.76 and 7.39 ppm of H in benzene of TBCSi as well as the peak of H in tert-butyl of TBCSi at 1.16 ppm, which indicates that TBCSi has been successfully joined to the three kinds of T-SSBR molecular chains ends respectively.

3.1.2. End-capping efficiency of T-SSBR

In the ^{1}H NMR spectra each characteristic peak area might be thought to stand for the H mol number of the group, and if the characteristic peak area is divided by H number of the group, the area occupied by 1 M H of the group (i.e., mole number of the group) will be obtained. Therefore, the ratio of the number of chain ends containing tert-butyldiphenylsilyl to total chain ends, i.e., the end-capping efficiency (E) could be calculated by the ratio of the peak areas of TBCSi-benzene H to SSBR-benzene H from the ^{1}H NMR spectra. The formula of end-capping efficiency is as follows,

$$E = \frac{S_{TBH}}{S_{SBH}} \times \frac{\frac{Mn}{Ms} \times St\% \times 5}{10 \times 2}$$

S_{TBH} and S_{SBH} respectively stand for the peak area of 10 H in TBCSi-benzene and 5 H in SSBR-benzene; Mn stands for the number-average molecular weight of the polymer; Ms stands for the molecular weight of Styrene; St% represents styrene content. The end-capping efficiency, calculated by the upper formula, is shown in Table 1.

3.2. Stress relaxation

The stress-relaxation curves and time of T-SSBR/CB and SSBR/CB compounds are shown in Fig. 3 and Table 2.

As seen from Fig. 3 and Table 2, all samples show a similar shape in stress-relaxation pattern, i.e., an initial period, where relaxation is linear and rapid with time, followed by a gradual steady zone of equilibrium plateau. The results are similar to the recent work of Djordjevic et al. [24]. In terms of the stress-relaxation rate, A_1 is the fastest, followed by A_4, which is faster than A_2 and A_3. It demonstrates the higher the SSBR-chain-end flexibility is, the shorter the stress-relaxation time is. It is proved that after the modification of large-volume functional groups, the free movement of the molecular chain ends is restrained, which makes the stress-relaxation rate slow. The stress-relaxation rate of A_2 is a little faster than that of A_3, because the molecular weight of A_2 is smaller than that of A_3. Moreover, the macromolecular chain flexibility of T_B-SSBR is superior to that of T_S-SSBR, whereas inferior to that of SSBR. Accordingly, the stress-relaxation time of A_4 lies between A_1 and A_2, which reveals that the more significant the immobilization of molecular end is, the slower the stress-relaxation rate is.

3.3. Rheological properties

Rheological properties of T-SSBR/CB and SSBR/CB compounds are shown in Fig. 4.

Fig. 4 (a) exhibits that the apparent viscosity (η_a) of the four kinds of compounds all decreases with increasing shear rate (γ), which indicates that the four kinds of compounds are all shear-thinning non-newtonian fluid. By contrast, the shear stress (τ) and η_a of A_1 are the lowest, η_a of A_2 is approximately the same as that of A_3, and η_a of A_4 lies between that of A_2 and A_3. This illustrates that it is the large-volume functional groups at the ends of SSBR molecular chains that makes molecular disentanglement difficult, appearing high flow energy consumption.

From Fig. 4 (b) it could be seen that the die-swell ratio (B) of A_1–A_4 compounds respectively increases with increasing γ. By contrast, B of A_1 compound is the smallest, A_2 compound is close to A_3 compound and the largest, and B of A_4 compound lies between that of A_1 and A_2. It shows that T-SSBR with longer stress-relaxation time could behave larger die swell. This is because the elastic deformation of T_S-SSBR fluid in the flow channel is not easy to recover.

3.4. Dynamic mechanical properties

3.4.1. Strain-sweep spectra

$G' \sim \varepsilon\%$ and tan $\delta \sim \varepsilon\%$ curves of T-SSBR/CB and SSBR/CB composites are shown in Fig. 5.

Fig. 5 (a) shows that the decreasing amplitude ($\Delta G'$) of G' with increasing strain ($\varepsilon\%$) is $A_1 > A_4 > A_3 > A_2$. This indicates that Payne effect of A_1 is the highest, that of A_2 is the lowest and that of A_3 is close to that of A_2 [25,26], which illustrates that CB disperses better in

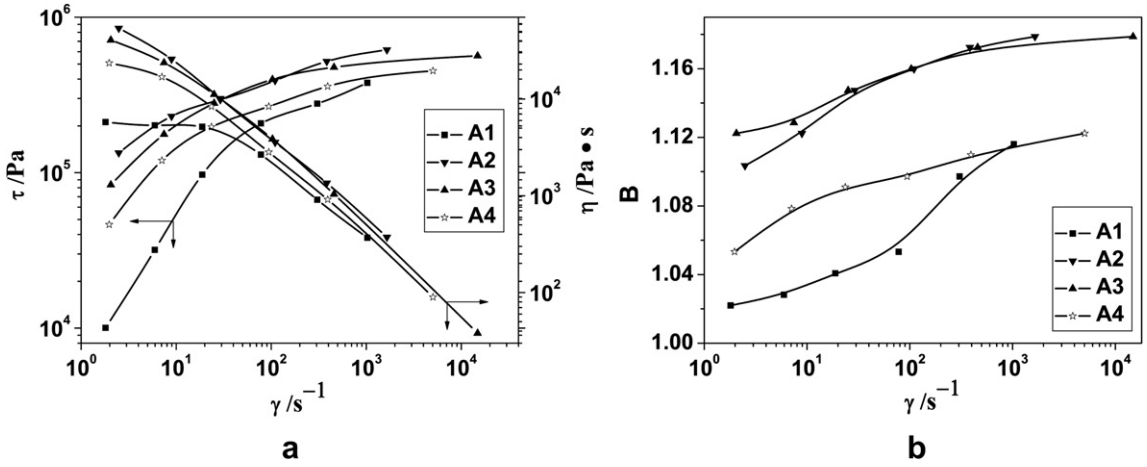

Fig. 4. τ,η and B vs γ curves of T-SSBR/CB and SSBR/CB compounds.

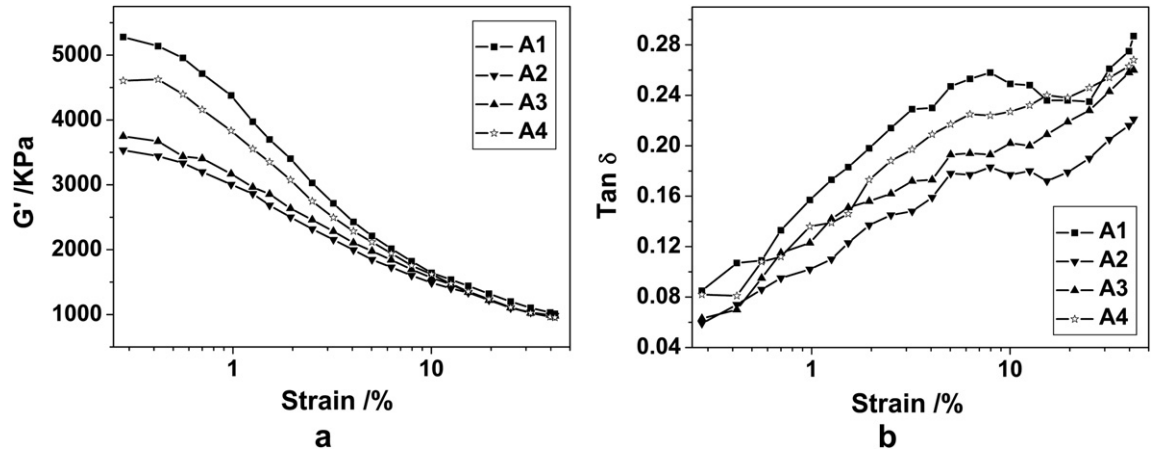

Fig. 5. G′ ~ ε% and tan δ ~ ε% curves of T-SSBR/CB and SSBR/CB composites.

T-SSBR than that in SSBR. This reveals that T-SSBR with 3–5 styrene unit and TBCSi at the end of molecular chains could enhance the adsorption to CB surface and improve CB dispersion in the rubber matrix.

Fig. 5 (b) displays that tan δ of A_1 increases with increasing ε% and presents one peak at about 10% strain, while A_2–A_4 are basically rising steadily. This may be because the larger CB aggregatesin A_1 composite are easy to breakdown at high ε%, leading to the decrease in G′ of A_1 composite, and then tan δ of A_1 composite increases again after 20% strain. Due to good CB dispersion, the internal friction of A_2–A_4 composites mainly results from the friction loss of molecular chains with increasing ε%. Compared with tan δ of A_1, that of A_2–A_4 composites are smaller, which indicates large-volume functional groups at the end of molecular chains immobilize the mobility of the free chain terminals and reduce the friction loss of the chain terminals. The tan δ of T-SSBR presents $A_2<A_3<A_4$ under the same strain, which indicates that the immobilization effect of T_S-SSBR is the most significant, leading to the remarkable decrease in the internal friction.

3.4.2. Temperature-sweep spectra

It is well known that hysteresis of tread composites, characterized by tan δ, at high temperature, is a key parameter which shows a good correlation with the rolling resistance of tires. On the other hand, it has been widely believed that the hysteresis at low temperature, related to the high-frequency nature of the dynamic strain involved in the skid process, is of importance. Therefore, lower tan δ at higher temperature (60 °C) and higher hysteresis at lower temperature (0 °C) will be favorable for both rolling resistance and wet-skid resistance [27]. The temperature dependence of tan δ and Tg of four kinds of SSBR composites with a constant frequency are shown in Fig. 6 and Table 3.

Generally, the temperature associated with the peak magnitude of the tan δ plot is defined as Tg [28]. From Fig. 6 and Table 3, Tg of A_2 is the lowest, which is related to its low St and Bv content. The structural parameters of A_3 and A_1 are similar, however, Tg of A_3 is higher than that of A_1, which shows that the molecular chain ends with large-volume functional groups could increase the transforming resistance of the chain segments from frozen state to high elastic state. Tan δ values of A_2–A_4 are higher than those of A_1 at 0 °C and lower than those of A_1 at 60 °C (i.e., the wet-skid resistance and rolling resistance of A_2–A_4 are superior to those of A_1). Among these the wet-skid resistance of T_S-SSBR (A_3) composites is the best. Therefore SSBR molecular chains end-capped by large-volume functional groups could significantly balance wet-skid resistance and rolling resistance.

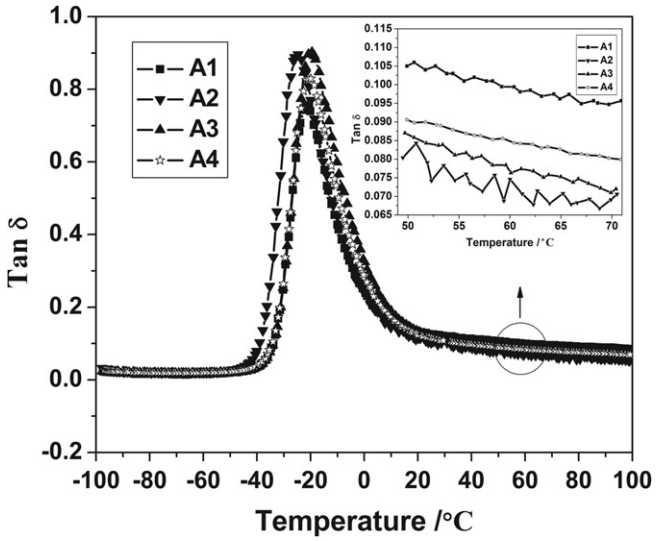

Fig. 6. Tan δ versus Temperature curves of T-SSBR/CB and SSBR/CB composites.

3.5. Vulcanizing and mechanical properties

Vulcanizing and mechanical properties of T-SSBR/CB and SSBR/CB composites are shown in Table 4.

The data in Table 4 show that the scorch time (t_{10}) and optimum cure time (t_{90}) of A_1–A_4 composites are similar, which indicates that TBCSi lying at the end of molecular chain has little effect on the vulcanizing characteristics of SSBR. The hardness of A_1 is the highest, which is related to the poor CB dispersion in SSBR. The tensile strength, elongation at break and tear strength of T-SSBR (A_2–A_4) composites are markedly higher than those of SSBR (A_1), owing to better CB dispersion in T-SSBR matrix. Compared with A_2, A_3 with higher molecular weight displays larger tensile strength, elongation at break and modulus at 300%. The tensile strength, modulus at

Table 3
Tg and tan δ of T-SSBR/CB and SSBR/CB composites.

Compound no.	A_1	A_2	A_3	A_4
Tg °C	−21.6	−24.6	−19.5	−20.9
tan δ (0 °C)	0.24	0.25	0.33	0.29
tan δ (60 °C)	0.10	0.07	0.08	0.08

Table 4
Vulcanizing and mechanical properties of T-SSBR/CB and SSBR/CB composites.

Compound no.	A_1	A_2	A_3	A_4
t_{10} (m:s)	4:47	4:09	4:05	4:29
t_{90} (m:s)	7:41	7:17	7:55	8:16
Shore A Hardness	75	71	73	74
Tensile strength (MPa)	15.5	17.3	19.0	18.2
Modulus at 300% (MPa)	12.9	12.6	13.3	12.3
Elongation at break (%)	351	384	413	414
Permanent set (%)	8	5	5	8
Tear strength (KNm^{-1})	32.8	33.7	33.1	32.9
Resilience (%)	31	47	40	38
Dynamic cutting resistance (g)	4.77	5.52	5.29	5.17
Compression heat build-up (°C)	15.1	11.0	12.5	13.5
Compression permanent set (%)	2.71	1.43	1.66	2.02

300% and tear strength of A_3 are bigger than those of A_4 although the structural parameters of A_3 and A_4 are similar, which illustrates that the remarkable immobilization of chain ends creates a greater degree of orientation in the force field, so the mechanical properties of T_S-SSBR are superior to those of T_B-SSBR [29]. The resilience of T-SSBR (A_2–A_4) is significantly higher than that of SSBR (A_1), and the compression heat build-up is lower than that of A_1. This is consistent with the lower internal friction of T-SSBR.

With regard to the dynamic cutting resistance A_1 is the best, followed by A_4, A_3 and A_2 in sequence. The dynamic cutting resistance is related to both stress-relaxation properties and molecular weight. A_1 composite with the shortest stress-relaxation time is easy to buffer the stress when suffering external forces, which is

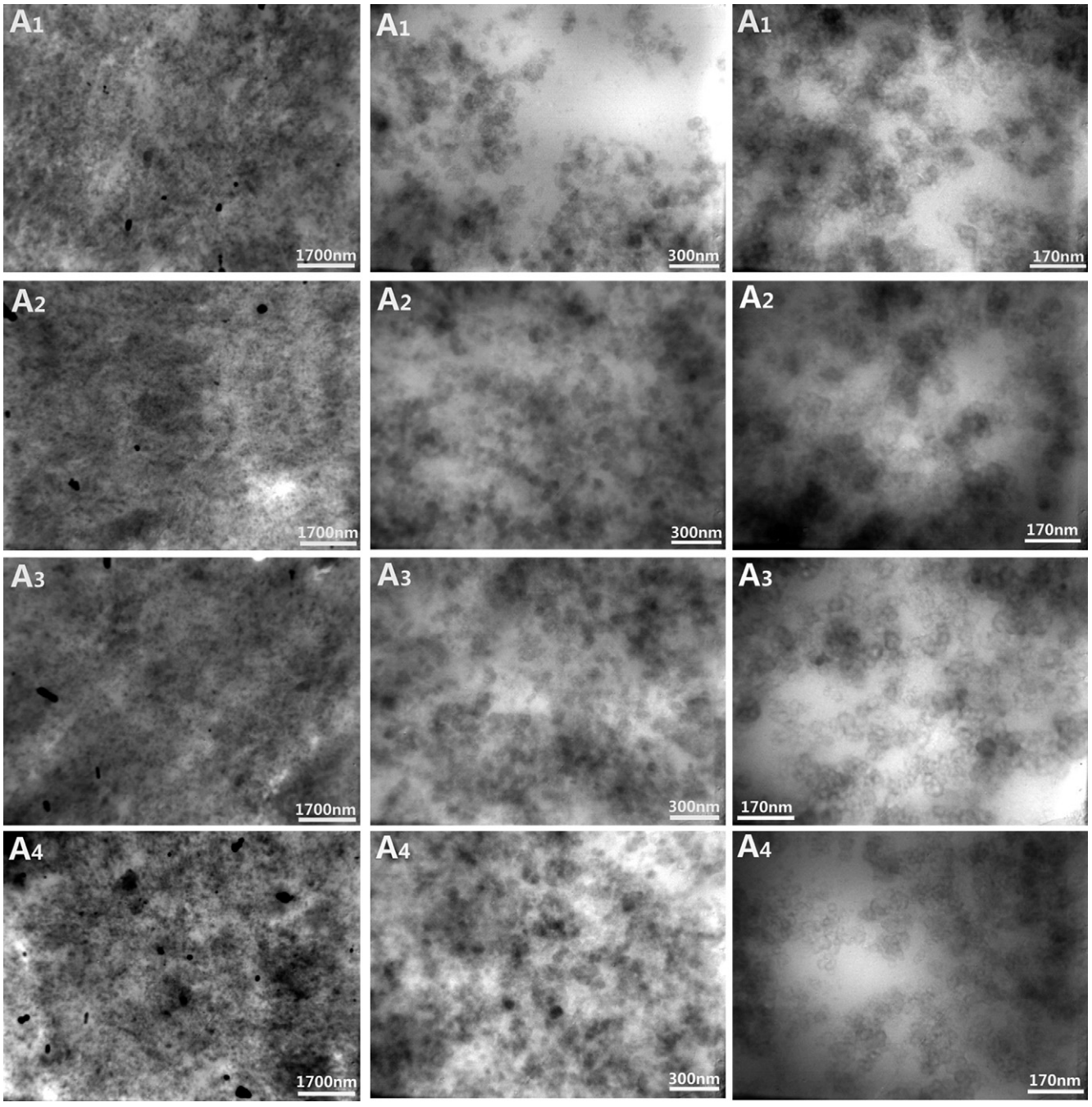

Fig. 7. TEM observations of T-SSBR/CB and SSBR/CB composites.

beneficial to improving the dynamic cutting resistance. The molecular weight presents $A_4>A_3>A_2$, therefore the dynamic cutting resistance exhibits $A_4>A_3>A_2$.

In short, large-volume functional groups, joining to the ends of SSBR molecular chains, contribute to not only the significant decrease in hardness, dynamic compression heat built-up and permanent set, but also the great improvement in mechanical properties and resilience of the SSBR composites. Whereas the dynamic cutting resistance of the T-SSBR/CB composites was slightly decreased.

3.6. Morphological structure of SSBR/CB composites

TEM photographs of T-SSBR and SSBR filled with CB are displayed in Fig. 7.

As shown clearly in Fig. 7, the light part presents the rubber matrix and the dark part is CB particles. Fig. 7 (A_1) shows that CB particles present obvious filler-network structure and agglomeration phenomenon, because the filler–filler interactions of the system are stronger than the filler–elastomer interactions. The TEM photographs of A_2, A_3 and A_4 show that the CB particle is slightly transparent with about 30 nm in diameter, which exhibits bead-chain distribution. As for the dispersion of CB in the rubber matrix, T-SSBR is better than SSBR and T_S-SSBR is better than T_B-SSBR. The results further reveal that SSBR molecular chains terminated with styrene unit and end-capped by large-volume functional groups have the strong adsorption for CB, which could efficiently make nano-fillers implement nano-dispersion in the matrix.

4. Conclusions

(1) SSBR with large-volume functional groups at the end of molecular chains could be prepared by adding TBCSi to SSBR solution at the end of anionic polymerization and reacting for an hour, and the end-capping efficiency of the obtained T-SSBR reaches 51–71%, which is calculated by the ratio of the peak areas of H in TBCSi-benzene to that in SSBR-benzene from the ^{1}H NMR spectra.

(2) The stress-relaxation time of the three kinds of T-SSBR is longer than that of SSBR and their die-swell ratios are larger than that of SSBR, which indicates that it is the large-volume functional group at the end of molecular chains that contributes the hindrance function to the motion of macromolecular chain. η_a of T-SSBR is larger than that of SSBR. Therefore, relative higher processing temperature is required for T-SSBR. By contrast, the hindrance function of T_B-SSBR is lower than that of T_S-SSBR.

(3) The dispersion of CB in T-SSBR is better than that in SSBR, i.e., Payne effects of T-SSBR are low and the dispersion of CB in T_S-SSBR is the best of all.

(4) T-SSBR/CB composites present low hardness and internal friction, high tensile strength, elongation at break, tear strength and resilience, and excellent balance between wet-skid resistance and rolling resistance. Furthermore, the comprehensive performances of T_S-SSBR are far superior to those of T_B-SSBR. Accordingly, the former is suitable for the tread material of green tires.

Acknowledgments

The authors gratefully acknowledge National Tenth-five Year Plan (2004 BA 310 A 41) and National Natural Science Foundation of China (50573005) financially supported.

References

[1] Liu X, Zhao SH. J Appl Polym Sci 2008;108:3038–45.
[2] Wang MJ, Lu SX, Mahmud K. J Polym Sci Pol Phys 2000;38(9):1240–9.
[3] Liu X, Zhao SH. J Appl Polym Sci 2008;109:3900–7.
[4] Bond R, Morton GF. Polymer 1984;25(1):132–40.
[5] Mosnácek J, Yoon JA, Juhari A, Koynov K, Matyjaszewski K. Polymer 2009;50(9):2087–94.
[6] Jaramillo-Soto G, García-Morán PR, Enríquez-Medrano FJ, Maldonado-Textle H, Albores-Velasco ME, Guerrero-Santos R, et al. Polymer 2009;50(21):5024–30.
[7] Passaglia E, Donati F. Polymer 2007;48(1):35–42.
[8] Halasa AF, Prentis J, Hsu B, Jasiunas C. Polymer 2005;46(12):4166–74.
[9] Nagata N, Kobatake T, Watanabe H, Ueda A, Yoshioka A. Rubber Chem Technol 1987;60(5):837–55.
[10] Tsutsumi F, Sakakibara M, Oshima N. Rubber Chem Technol 1990;63(1):8–22.
[11] Bortolotti M, Busetti S, Mistrali F, Soddu L, Vitalini L. Kautsch Gummi Kunstst 1998;51(5):331–5.
[12] Kobayashi N, Tadaki T, Akema H. Jpn Kokai Tokkyo Koho; 2000, EP 1000970B1.
[13] Sierra CA, Galan C, Gomez FJM. Rubber Chem Technol 1995;68(2):259–66.
[14] Kawanaka T, Watanabe H. US 5001 196; 1991.
[15] Ueda A, Akita S, Namizuka T. US 4555 547; 1985.
[16] Ueda A, Akita S, Chida T. US 4555 548; 1985.
[17] Wang Z, Zhao SH, Zhang JM. China Rubber Industry 1999;46(7):425–30.
[18] Duan YX, Zhao SH, Zhang XY, Zhang TY. China Rubber Ind 2002;49(11):645–9.
[19] Hao YQ, Wang YF, Yan TL, Yao M, Feng HD, Liu X, et al. Sino-Global Energy 2007;12(5):90–3.
[20] Liu X, Zhao SH, Zhang XY, Li XL, Bai Y. China Synth Rubber Ind 2008;31(6):482.
[21] Li XL, He ML, Zhang XY, Yao M. China Synth Rubber Ind 2008;31(2):155.
[22] Morita K. Jpn Kokai Tokkyo Koho 1999; JP 349 632.
[23] Kim E, Lee E, Park I, Chang T. Polym J 2002;34(9):674–81.
[24] Djordjevic I, Choudhury NR, Dutta NK, Kumar S. Polymer 2009;50(7):1682–91.
[25] Payne AR. J Appl Polym Sci 1962;6:57–63.
[26] Payne AR, Whittaker RE. Rubber Chem Technol 1971;44(2):440–78.
[27] Wang MJ. Rubber Chem Technol 1998;71(3):520–89.
[28] Yang ZL, Wicks DA, Hoyle CE, Pu HT, Yuan JJ, Wan DC, et al. Polymer 2009;50(7):1717–22.
[29] Sarva SS, Hsieh AJ. Polymer 2009;50(13):3007–15.